

Solvent-Dependent Intramolecular Electron Transfer in a Peptide-Linked $[\text{Ru}(\text{bpy})_3]^{2+}-\text{C}_{60}$ Dyad

Alessandra Polese,[†] Simonetta Mondini,[‡] Alberto Bianco,[‡] Claudio Toniolo,[†] Gianfranco Scorrano,[‡] Dirk M. Guldi,^{*,§} and Michele Maggini^{*,‡}

Contribution from the Centro Meccanismi Reazioni Organiche and Centro Studio Biopolimeri del CNR, Dipartimento di Chimica Organica, Università di Padova, Via Marzolo 1, 35131 Padova, Italy, and Radiation Laboratory, University of Notre Dame, Notre Dame, Indiana 46656

Received September 25, 1998

Abstract: A novel peptide-linked $[\text{Ru}(\text{bpy})_3]^{2+}-\text{C}_{60}$ dyad is shown to undergo an intramolecular photoinduced electron transfer in chlorinated hydrocarbons that causes quenching of the emission associated to the ruthenium metal-to-ligand charge-transfer excited state. Addition of a strong protic solvent, such as hexafluoro-2-propanol, leads to deactivation of the electron-transfer process with concomitant recovery of the emission to the extent recorded for a solution of a reference ruthenium complex lacking the fullerene moiety. This behavior is associated with a direct effect of the protic solvent on the secondary structure of the peptide spacer, whose preferred conformations in solution have been assessed by FT-IR and 2D NMR spectroscopy. Chlorinated hydrocarbons favor the peptide 3_{10} -helical conformation, which provides efficient interactions between the ruthenium and C_{60} chromophores, whereas the presence of a protic solvent produces helix unfolding, which hampers suitable spatial orientations of the chromophores for electron transfer. The reversibility of the phenomenon is also demonstrated and discussed.

Introduction

Intramolecular energy- or electron-transfer processes within polypeptide-bridged donor–acceptor (D–A) systems have been the subject of extensive theoretical and experimental studies.¹ Short peptides of different main-chain lengths, especially those rich in the structurally restricted C^α -tetrasubstituted α -amino acid Aib (α -aminoisobutyric acid), have been used as molecular rulers to separate the redox partners covalently attached to their N- and C-termini^{1b,2} or incorporated within the sequence as side-chain-modified amino acids.³ An attractive feature of peptide-based interchromophore bridges is that transitions between the peptide secondary structures, induced by temperature or solvent changes, can be profitably exploited to modulate the extent of interactions between the D and A units.⁴ In this paper, we report the synthesis and the photophysical behavior of a $[\text{Ru}(\text{bpy})_3]^{2+}$ –hexapeptide– C_{60} (bpy = 2,2'-bipyridine) system in which a photoinduced electron transfer and the related metal-to-ligand charge transfer (MLCT) excited-state luminescence signal are switched on/off by a conformational transition of the secondary

structure of the peptide spacer. The $[\text{Ru}(\text{bpy})_3]^{2+}$ unit was chosen as the photoactive electron donor center because of the long lifetime and high-lying energy of the redox-active ruthenium(II) MLCT excited state, whose prominent emission above 610 nm is produced with high quantum efficiency.⁵ The [60]-fullerene core was selected owing to its remarkable electron acceptor properties in both the ground and excited states⁶ and its low reorganization energy,⁷ and because C_{60} radical anions are stable species that can be accurately characterized by spectroscopic methods.⁷ In chlorinated hydrocarbons, the hexapeptide spacer adopts a 3_{10} -helical structure (the distance between

(5) (a) Yersin, H.; Vogler, A.; Eds. *Photochemistry and Photophysics of Coordination Compounds*; Springer: Berlin, 1987. (b) Juris, A.; Balzani, V.; Barigelletti, F.; Campagna, S.; Belser, P.; Zelewsky, A. *Coord. Chem. Rev.* **1988**, *84*, 85. (c) Collin, J. P.; Guillerez, S.; Sauvage, J. P.; Barigelletti, F.; Flamigni, L.; De Cola, L.; Balzani, V. *Coord. Chem. Rev.* **1991**, *111*, 291. (d) Horvath, O.; Stevenson K. L.; Eds. *Charge-Transfer Photochemistry*; VCH: Weinheim, 1993. (e) Balzani, V.; Juris, A.; Venturi, M.; Campagna, S.; Serroni, S. *Chem. Rev.* **1996**, *96*, 759.

(6) (a) Sariciftci, N. S.; Smilowitz, L.; Heeger, A. J.; Wudl, F. *Science* **1992**, *258*, 1474. (b) Williams, R. M.; Verhoeven, J. W. *Chem. Phys. Lett.* **1992**, *194*, 446. (c) Wang, Y. *Nature* **1992**, *356*, 585. (d) Arbogast, J. W.; Darmanian, A. P.; Foote, C. S.; Rubin, Y.; Diederich, F.; Alvarez, M. M.; Anz, S. J.; Whetten, R. L. *J. Phys. Chem.* **1991**, *95*, 11.

(7) (a) Imahori, H.; Sakata, Y. *Adv. Mater.* **1997**, *9*, 537 and references therein. (b) Prato, M. *J. Mater. Chem.* **1997**, *7*, 1097. (c) Liddell, P. A.; Kuciauskas, D.; Sumida, J. P.; Nash, B.; Nguyen, D.; Moore, A. L.; Moore T. A.; Gust, D. *J. Am. Chem. Soc.* **1997**, *119*, 1400. (d) Sun, Y.; Drovetskaya, T.; Bolskar, R. D.; Bau, R.; Boyd, P. D. W.; Reed, C. A. *J. Org. Chem.* **1997**, *62*, 3642. (e) Guldi, D. M.; Maggini, M.; Scorrano, G.; Prato, M. *J. Am. Chem. Soc.* **1997**, *119*, 974. (f) Baran, P. S.; Monaco, R. R.; Khan, A. U.; Schuster, D. I.; Wilson, S. R. *J. Am. Chem. Soc.* **1997**, *119*, 8363. (g) Imahori, H.; Yamada, K.; Hasegawa, M.; Taniguchi, S.; Okada, T.; Sakata, Y. *Angew. Chem., Int. Ed. Engl.* **1997**, *36*, 2626. (h) Sakata, Y.; Imahori, H.; Tsue, H.; Higashida, S.; Akiyama, T.; Yoshizawa, E.; Aoki, M.; Yamada, K.; Hagiwara, K.; Taniguchi, S.; Okada, T. *Pure Appl. Chem.* **1997**, *69*, 1951. (i) Martin, N.; Perez, I.; Sanchez, L.; Seoane, C. *J. Org. Chem.* **1997**, *62*, 5690. (j) Armaroli, N.; Diederich, F.; Dietrich-Buchecker, C. O.; Flamigni, L.; Marconi, G.; Nierengarten, J.-F.; Sauvage, J.-P. *Chem. Eur. J.* **1998**, *4*, 406.

[†] Centro Biopolimeri-CNR, University of Padova.

[‡] Centro Meccanismi-CNR, University of Padova.

[§] Radiation Laboratory, University of Notre Dame.

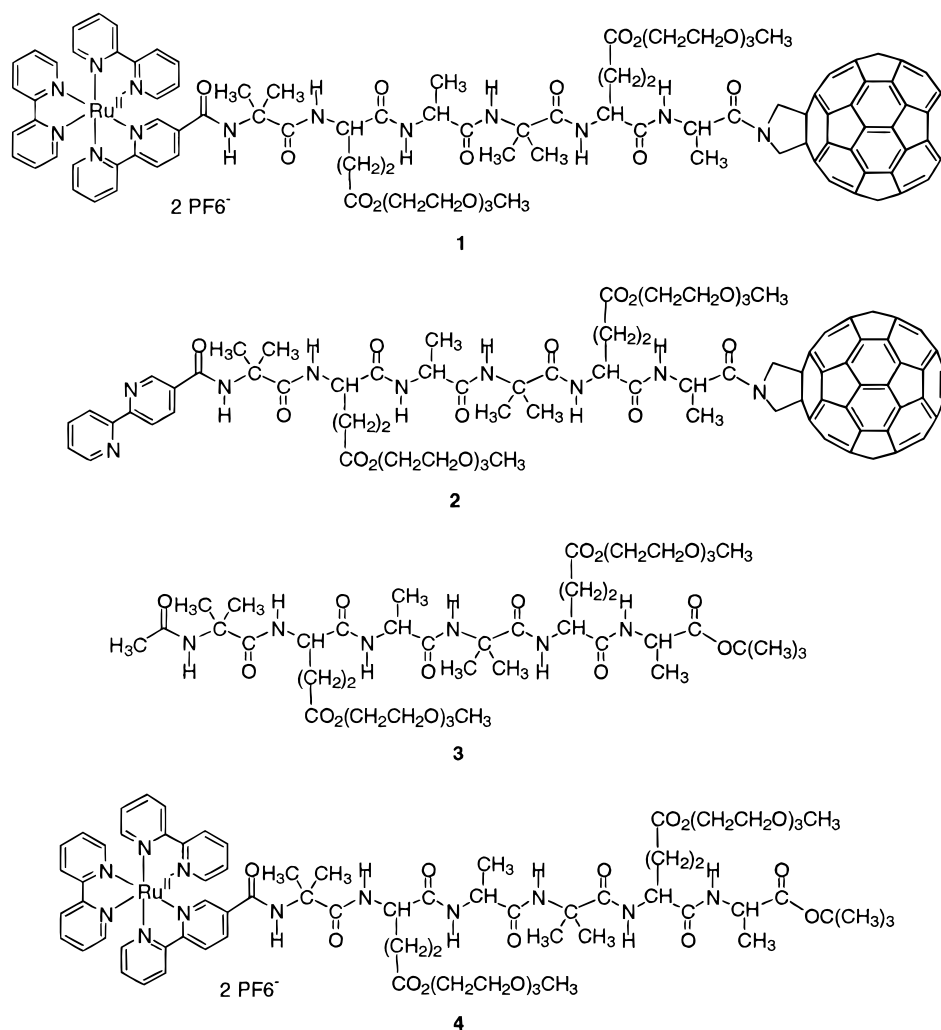
(1) (a) Voyer, N.; Lamothe, J. *Tetrahedron* **1995**, *51*, 924. (b) Isied, S. S.; Ogawa, M. Y.; Wishart, J. F. *Chem. Rev.* **1992**, *92*, 381. (c) Fox, M. A. *Acc. Chem. Res.* **1992**, *25*, 569.

(2) Fernando, S. R. L.; Kozlov, G. V.; Ogawa, M. Y. *Inorg. Chem.* **1998**, *37*, 1900 and references therein.

(3) (a) Basu, G.; Kubasik, M.; Anglos, D.; Secor, B.; Kuki, A. *J. Am. Chem. Soc.* **1990**, *112*, 9410. (b) Basu, G.; Anglos, D.; Kuki, A. *Biochemistry* **1993**, *32*, 3067. (c) Anglos, D.; Bindra, V.; Kuki, A. *J. Chem. Soc., Chem. Commun.* **1994**, 213. (d) Slate, C. A.; Striplin, D. R.; Moss, J. A.; Chen, P.; Erickson, B. W.; Meyer, T. J. *J. Am. Chem. Soc.* **1998**, *120*, 4885. (e) Galoppini, E.; Fox, A. M. *J. Am. Chem. Soc.* **1996**, *118*, 2299. (f) Fox, A. M.; Galoppini, E. *J. Am. Chem. Soc.* **1997**, *119*, 5277.

(4) (a) Donald, F.; Hungerford, G.; Birch, D. J. S.; Moore, B. D. *J. Chem. Soc., Chem. Commun.* **1995**, 313. (b) Hungerford, G.; Martinez-Insua, M.; Birch, D. J. S.; Moore, B. D. *Angew. Chem., Int. Ed. Engl.* **1996**, *35*, 326.

Chart 1



the N- and C- termini is within 11–12 Å,⁸ which locates the ruthenium and C_{60} moieties in a favorable position for intramolecular MLCT luminescence quenching to the Ru^{3+} - C_{60}^{-} charge-separated pair. However, addition of 1,1,1,3,3,3-hexafluoro-2-propanol (HFIP) promotes a conformational transition of the peptide backbone with concomitant full recovery of the luminescence to the extent exhibited by a reference ruthenium complex lacking the electron-accepting fullerene moiety. More interestingly, the secondary structure's interconversion is fully reversible.^{4b} A luminescence spectrum, superimposable on that recorded in the chlorinated solvent prior to HFIP addition, was obtained upon removal of HFIP.

Results and Discussion

Synthesis. The hexapeptide spacer of dyad **1** (Chart 1) is characterized by the presence of two Aib residues, known to strongly induce a helical bias,⁹ in positions 1 and 4.

For solubility reasons, the two Glu residues, at positions 2 and 5 in the sequence, were side-chain functionalized with a triethyleneglycol chain. Scheme 1 illustrates the synthetic route that afforded ligand **2**, the precursor to dyad **1** through coordination to ruthenium(II). The free carboxylic acid of the N^{α} -bpy-blocked pentapeptide **6**, prepared by standard solution

procedures (see Supporting Information), was activated with EDC/HOAt¹⁰ (EDC = *N*-ethyl-*N'*-(3-dimethylaminopropyl)-carbodiimide; HOAt = 7-aza-1-hydroxybenzotriazole) and coupled to H-Ala-fulleropyrrolidine. The latter compound was synthesized by trifluoroacetic acid (TFA) hydrolysis of Boc-Ala-fulleropyrrolidine **5** (Boc = *tert*-butyloxycarbonyl), prepared in turn by treating fulleropyrrolidine¹¹ with the symmetrical anhydride (Boc-Ala)₂O.

Dyad **1** was synthesized by coordinating ligand **2** to ruthenium, using $Ru(bpy)_2Cl_2$ in refluxing 1,2-dichloroethane (DCE) in the presence of excess NH_4PF_6 ¹² (in 33% isolated yield from **2**). Compound **1** is reasonably soluble in CH_2Cl_2 , DCE, and CH_3CN , while it is insoluble in toluene. It was characterized by ¹H NMR, FT-IR (see Supporting Information), and UV-vis absorption spectroscopies. UV-vis absorption data indicate that no mutual interactions occur through the spacer between the electron donor (ruthenium) and the electron acceptor (fullerene) in the ground state. The MALDI mass spectrum shows a cluster of signals with a maximum at 2223 *m/z*, corresponding to the mass expected for dyad **1** after loss of two hexafluorophosphate units.

Hexapeptide **3** and the $[Ru(bpy)_3]^{2+}$ -hexapeptide **4** were synthesized starting from the hexapeptide Z-Aib-Glu(OTeg)-

(10) Carpino, L. A. *J. Am. Chem. Soc.* **1993**, *115*, 4397.

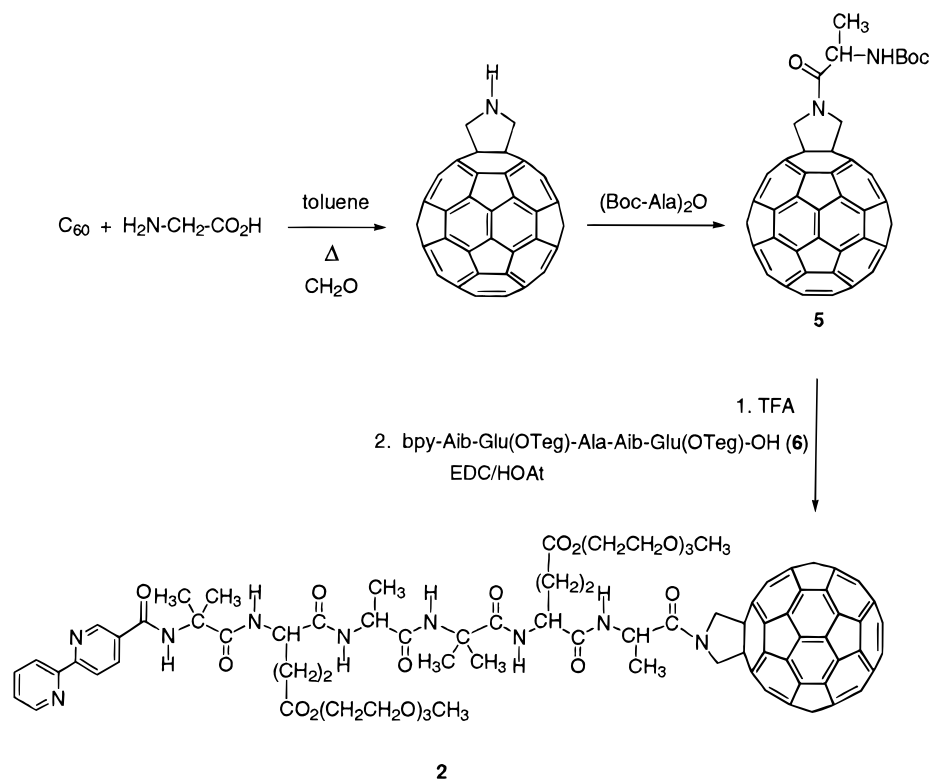
(11) Prato, M.; Maggini, M.; Giacometti, C.; Scorrano, G.; Sandonà G.; Farnia, G. *Tetrahedron* **1996**, *52*, 5221.

(12) Maggini, M.; Donò A.; Scorrano, G.; Prato, M. *J. Chem. Soc., Chem. Commun.* **1995**, 845.

(8) Toniolo, C.; Benedetti, E. *Trends Biochem. Sci.* **1991**, *16*, 350.

(9) (a) Karle, I. L.; Balaram, P. *Biochemistry* **1990**, *29*, 6747. (b) Toniolo, C.; Benedetti, E. *Macromolecules* **1991**, *24*, 4004.

Scheme 1



Ala-Aib-Glu(OTeg)-Ala-OrBu (see Supporting Information) and used as model compounds, together with ligand **2**, for conformational studies and the photophysical characterization of dyad **1**.

Solution Conformational Analysis. The solution conformation of the hexapeptide reference compound **3** was investigated by using a combination of FT-IR absorption and NMR techniques. In the N-H stretching region, the FT-IR spectra, recorded in CDCl₃ in the 10–0.1 mM concentration range, show a strong absorption band at 3320 cm⁻¹ and a weak band at 3434 cm⁻¹, assigned to H-bonded and free NH groups, respectively,^{13a} (see Supporting Information). The relative intensity of these bands is concentration independent. The hydrogen-bonding effect is that arising from intramolecular N-H···O=C interactions, as confirmed by the complementary stretching band at 1664 cm⁻¹, typical of the carbonyl absorption of helical peptides.^{13b} Additional information was obtained by titration of the peptide NH protons using ¹H NMR. The NH chemical shift analysis was performed upon addition of increasing amounts of the free radical 2,2,6,6-tetramethylpiperidine-1-oxyl (TEMPO)¹⁴ to a CDCl₃ solution of peptide **3**. Two classes of protons were found (Figure 1A): the first class includes two protons (Aib¹ NH and Glu² NH, unambiguously assigned by 2D NMR experiments), very sensitive to the addition of TEMPO, while the second class includes the four remaining intramolecularly bonded protons, whose chemical shifts are almost unaffected by addition of the free radical. These observations suggest that the ordered secondary structure adopted in solution by peptide **3** is the 3₁₀-helix.¹⁵

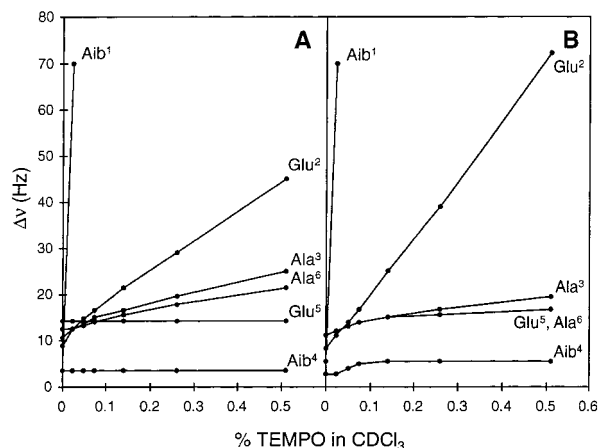


Figure 1. Plot of the bandwidth of the NH protons of model peptides **3** (A) and **2** (B) as a function of increasing percentages of TEMPO (w/v) added to the CDCl₃ solution. Peptide concentration, 1 mM.

The FT-IR absorption study performed on ligand **2** gave results superimposable on those found for model **3**, while NMR conformational experiments confirmed that the ordered secondary structure holds also in the presence of a combination of the bpy and fullerene moieties (Figure 1B). These findings are in line with an early report by some of us on a methanofullerene derivative, covalently linked to a pentapeptide framework, whose 3₁₀-helical structure was not influenced by C₆₀.¹⁶

To confirm these results, complementary 2D NMR (TOCSY, NOESY, and ROESY) experiments were carried out in both CDCl₃ and DMSO-*d*₆ for model hexapeptide **3** but, for solubility reasons, only in CDCl₃ for ligand **2**. Besides the complete assignment of all proton resonances, from this latter study we found a series of sequential NH–NH (*i* → *i* + 1) and some

(13) (a) Bonora, G. M.; Mapelli, C.; Toniolo, C.; Wilkening, R. R.; Stevens, E. S. *Int. J. Biol. Macromol.* **1984**, *6*, 179. (b) Kennedy, D. F.; Crisma, M.; Toniolo, C.; Chapman, D. *Biochemistry* **1991**, *30*, 6541.

(14) Kopple, K. D.; Schamper, T. J. *J. Am. Chem. Soc.* **1972**, *94*, 3644.

(15) Toniolo, C.; Bonora, G. M.; Barone, V.; Bavoso, A.; Benedetti, E.; Di Blasio, B.; Grimaldi, P.; Lelj, F.; Pavone, V.; Pedone, C. *Macromolecules* **1985**, *18*, 895.

(16) Prato, M.; Bianco, A.; Maggini, M.; Scorrano, G.; Toniolo, C.; Wudl, F. *J. Org. Chem.* **1993**, *58*, 5578.

Table 1. Inter-residue NOE Correlations for Model Peptides **2** and **3**

bpy-[Aib-Glu(OTeg)-Ala] ₂ -fulleropyrrolidine 2 ,		Ac-[Aib-Glu(OTeg)-Ala] ₂ -OrBu 3	
CDCl ₃	CDCl ₃ and DMSO- <i>d</i> ₆ 1:1	CDCl ₃ /HFIP- <i>d</i> ₂	
$d_{\text{NN}} i \rightarrow i + 1$	$d_{\text{NN}} i \rightarrow i + 1$	$d_{\text{NN}} i \rightarrow i + 1$	
Aib ¹ HN-Glu ² HN	Aib ¹ HN-Glu ² HN	—	
Glu ² HN-Ala ³ HN	Glu ² HN-Ala ³ HN	—	
Ala ³ HN-Aib ⁴ HN	Ala ³ HN-Aib ⁴ HN	Ala ³ HN-Aib ⁴ HN	
Aib ⁴ HN-Glu ⁵ HN	Aib ⁴ HN-Glu ⁵ HN	—	
Glu ⁵ HN-Ala ⁶ HN	Glu ⁵ HN-Ala ⁶ HN	—	
$d_{\alpha\text{N}} i \rightarrow i + 1$	$d_{\alpha\text{N}} i \rightarrow i + 1$	$d_{\alpha\text{N}} i \rightarrow i + 1$	
—	Ala ³ H α -Aib ⁴ HN	—	
Glu ⁵ H α -Ala ⁶ HN	Glu ⁵ H α -Ala ⁶ HN	—	
$d_{\alpha\text{N}} i \rightarrow i + 2$	$d_{\alpha\text{N}} i \rightarrow i + 2$	$d_{\alpha\text{N}} i \rightarrow i + 2$	
—	Glu ² H α -Aib ⁴ HN	—	
Ala ³ H α -Glu ⁵ HN	Ala ³ H α -Glu ⁵ HN	—	
$d_{\alpha\text{N}} i \rightarrow i + 3$	$d_{\alpha\text{N}} i \rightarrow i + 3$	$d_{\alpha\text{N}} i \rightarrow i + 3$	
Ala ³ H α -Ala ⁶ HN	Ala ³ H α -Ala ⁶ HN	—	

long-range $\alpha\text{H-NH}$ ($i \rightarrow i + 2$) NOE interactions, typical of a 3_{10} -helix conformation (Table 1).¹⁷

Direct NMR conformational experiments on dyad **1** were hampered by the presence of the ruthenium trisbipyridine proton resonances that precluded (i) a meaningful TEMPO-dependent NH chemical shift study and (ii) the interpretation of the 2D NMR data. Although the conformational characterization would have been performed on reference compound **3** and on bpy-hexapeptide-C₆₀ **2**, the closest precursor to dyad **1**, it is reasonable to assume that the ruthenium complex should not interfere with the 3_{10} -helical structure adopted in solution by the peptide spacer.

Luminescence Studies of Compounds 1 and 4 in Chlorinated Hydrocarbons. Steady-state luminescence of **1** (2×10^{-5} M) in degassed CH₂Cl₂ or 1-chlorobutane (CBT) exhibits a significant reduction in intensity, relative to the reference [Ru(bpy)₃]²⁺-hexapeptide complex **4** lacking the C₆₀ moiety. The latter shows, as in general all of the Ru(II) trisbipyridine complexes, a very strong luminescence associated with the MLCT excited state, which is long-lived (lifetime = 220 ns).

Determination of the dynamics associated with the rapid quenching of the MLCT excited state in **1** were investigated by picosecond-resolved transient absorption experiments. In sharp contrast to reference compound **4**, photolysis of dyad **1** reveals that the initially formed MLCT excited state, with its characteristic bleaching at wavelengths above 600 nm, decays rapidly (lifetime = 2.9 ns). This transformation leads to the grow-in of a new absorption at about 520 nm, which differs substantially from those found for the fullerene singlet or triplet excited states. Complementary nanosecond experiments in the UV-vis and near-IR regions were performed to characterize the nature and fate of the transients produced during the picosecond time regime. Differential absorption changes of dyad **1** in CH₂Cl₂, recorded 50 ns after an 8 ns laser pulse excitation (337 nm), are similar to those monitored during the picosecond time regime (Figure 2).¹⁸

Furthermore, near-IR measurements revealed the rapid generation of a new transition near 1000 nm (Figure 3). Since the latter absorption is a characteristic signature for the fullerene radical anion,⁷ we assign the product evolving from intramolecular MLCT quenching to the Ru³⁺-C₆₀^{•-} charge-separated pair.

(17) Wütrich, K. *NMR of Proteins and Nucleic Acids*; Wiley: New York, 1986.

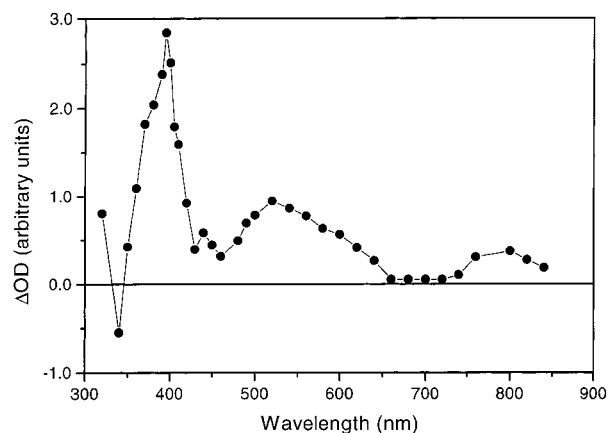


Figure 2. Differential absorption spectrum obtained upon flash photolysis of dyad **1** (2×10^{-5} M) in CH₂Cl₂ with an 8 ns laser pulse (337 nm) at 25 °C: UV-vis part recorded 50 ns after excitation.

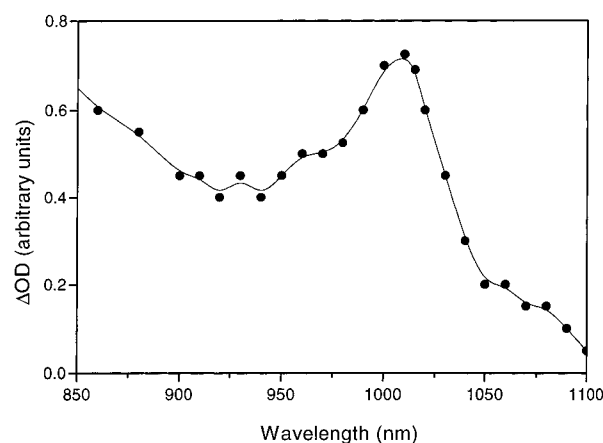


Figure 3. Differential absorption spectrum obtained upon flash photolysis of dyad **1** (2×10^{-5} M) in CBT with an 8 ns laser pulse (337 nm) at 25 °C: near-IR part recorded 100 ns after excitation.

Luminescence Studies in Protic Solvents: Denaturation of Peptide Spacer in Dyad 1. Protic solvents, in particular fluoro alcohols, are known to often unfold short helical peptides owing to their ability to effectively compete with N-H...O=C intramolecular hydrogen bonding as donors.^{3f,19} Upon addition of ethanol, 2,2,2-trifluoroethanol (TFE), and HFIP to a solution of dyad **1** in CBT, the strongly quenched luminescence of the ruthenium MLCT excited state gradually increases relative to that of the reference ruthenium complex **4** (Figure 4). In particular, addition of HFIP up to a 1:1 (v/v) CBT/HFIP ratio leads to a full recovery of luminescence to the extent recorded for a solution of **4** in 1:1 CBT/HFIP.²⁰

Emission yields of dyad **1** in CBT, in the presence and in the absence of HFIP, were compared to those of the dyads

(18) It should be noted that the absorption characteristics of dyad **1** are the sum of the absorptions of the ruthenium(II) trisbipyridine complex and C₆₀ chromophores. Thus, laser irradiation, for example at 337 nm, leads, besides excitation of the ruthenium antenna, eventually to the formation of the fullerene excited triplet state. This prompted us to correct the observed differential absorption changes for the contribution of the fullerene excited triplet state. Pulse reduction of bpy-hexapeptide-C₆₀ **2** and oxidation of [Ru(bpy)₃]²⁺-hexapeptide **4** was used for the interpretation of the spectral features in the UV-vis range (Figure 2) found for the charge-separated state of dyad **1**. The strong band of the fullerene radical anion (near 420 nm) masks the ruthenium-related bleaching (near 440 nm). In turn, bleaching of ground-state fullerene (near 335 nm) is compensated for by the sharp absorption of the ruthenium(III) complex in this same wavelength range (ref 21).

(19) (a) Toniolo, C.; Bonora, G. M.; Fontana, A. *Int. J. Pept. Protein Res.* **1974**, *6*, 371. (b) Hanson, P.; Millhauser, G.; Formaggio, F.; Crisma, M.; Toniolo, C. *J. Am. Chem. Soc.* **1996**, *118*, 7618.

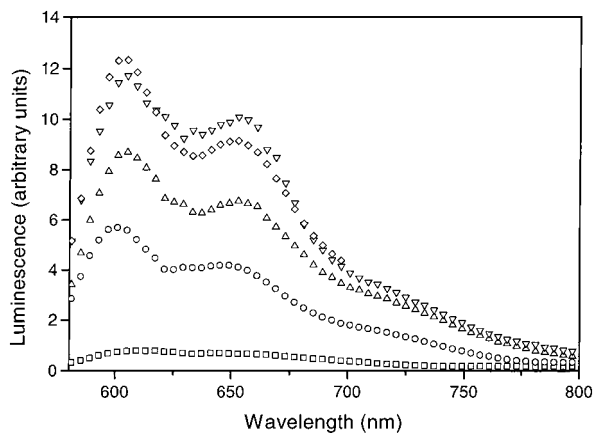
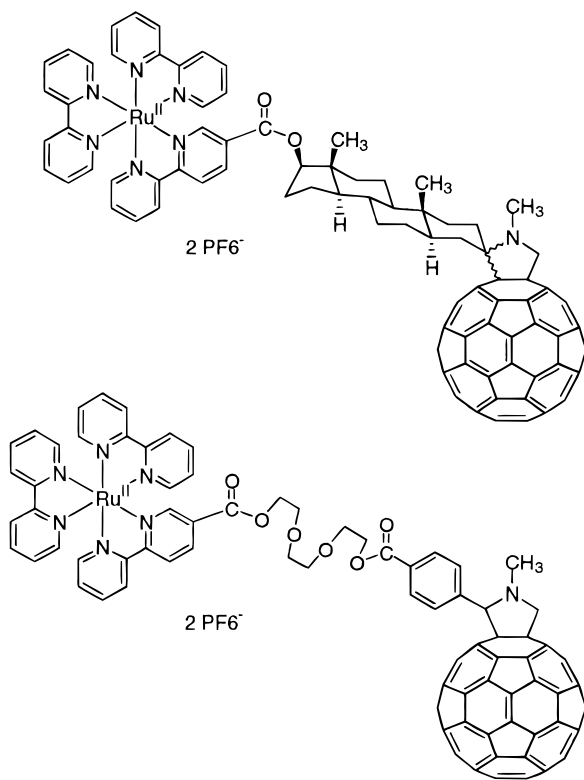


Figure 4. Emission spectra (excitation at 460 nm) of dyad **1** in CBT (□), in 1:1 CBT/EtOH (○), in 1:1 CBT/TFE (△), and in 1:1 CBT/HFIP (◇) and of reference ruthenium complex **4** in 1:1 CBT/HFIP (▽) at 77 K. As all samples were studied under identical conditions, the relative intensities represent relative emission quantum yields.

Chart 2



shown in Chart 2, in which ruthenium and C₆₀ are spaced by a rigid androstane²¹ or a flexible triethyleneglycol bridge,^{12,22} respectively.

We found that addition of HFIP leads to a strong decrease of the luminescence intensity for both dyads, thus corroborating

(20) The intermediate values of luminescence (Figure 4) can be related to a progressive collapse of the peptide helical structure induced by the addition of the protic cosolvent to CBT. The picosecond absorption decay profile in pure CBT is monoexponential, whereas upon addition of HFIP the profile becomes multiexponential. In principle, the decay of the transients absorption can be used to shed light on changes of the peptide backbone conformational state. However, the presence of different peptide conformer populations is overshadowed by the photophysical processes of the ruthenium and C₆₀ chromophores. It is a general belief, however, that, in solution, families of conformers simultaneously exist in equilibrium. Therefore, the presence of a heterogeneous mixture of conformers in CBT/protic cosolvent cannot be ruled out.

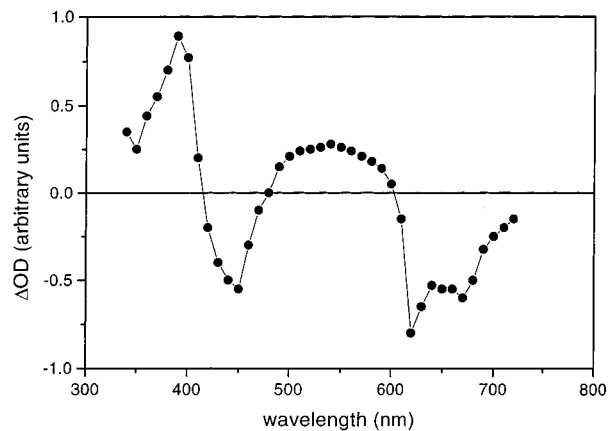


Figure 5. Differential absorption spectrum obtained upon flash photolysis of dyad **1** (2×10^{-5} M) in 1:1 CBT/HFIP with an 8 ns laser pulse (337 nm) at 25 °C.

the assumption that the observed solvent-responsive behavior of the luminescence intensity for **1** is a direct effect of HFIP on the secondary structure of the peptide spacer.²³ 2D NMR experiments (Table 1) were performed on model hexapeptide **2** dissolved in a 1:1 CDCl₃/HFIP-*d*₂ mixture. Again, we could assign all proton resonances, but, in contrast to the experiments in neat CDCl₃, we could not observe any characteristic NH–NH (*i* → *i* + 1) correlation, typical of helical conformations.¹⁷

From both the luminescence and 2D NMR studies, we conclude that the peptide spacer of dyad **1** adopts a 3₁₀-helical structure in chlorinated hydrocarbons, while in the presence of a strong protic solvent, such as HFIP, the helical conformation tends to collapse.¹⁹

Nanosecond photolysis of dyad **1** in a 1:1 CBT/HFIP solvent mixture reveals the instantaneous formation of a transient absorption (Figure 5), which decays with a lifetime of 535 ns.

This transient is predominantly emissive in the 420–480 nm region and also above 600 nm. The earlier bleaching (420–480 nm) correlates well with the MLCT ground-state absorption and indicates conversion of the antenna ground state to the excited state. In contrast, the latter (600 nm) originates from the strong luminescence of the MLCT excited state. The lifetime of this emission (535 ns) is, however, longer than that noticed for model compound **4** (220 ns). More importantly, the monitored wavelength fails to provide spectral evidence which would be in support of the formation of a Ru³⁺–C₆₀^{•-} radical pair. This confirms that addition of HFIP has a key function of blocking the intramolecular electron-transfer process.

On a longer time scale (2 μs after the laser pulse), the detected differential absorption features are typical of the excited triplet state of fulleropyrrolidines. The triplet quantum yield, close to that determined in neat CBT, indicates a direct excitation of the fullerene moiety in dyad **1**. This finding rules out energy transfer from the ruthenium MLCT to the C₆₀ unit as a major contribution to the overall deactivation processes of photoexcited **1**. On the other hand, deactivation of the fullerene excited singlet

(21) Maggini, M.; Guldi, D. M.; Mondini, S.; Scorrano, G.; Paolucci, F.; Ceroni, P.; Roffia, S. *Chem. Eur. J.* **1998**, *4*, 1992.

(22) Sariciftci, N. S.; Wudl, F.; Heeger, A. J.; Maggini, M.; Scorrano, G.; Prato, M.; Bourassa, J.; Ford, P. C. *Chem. Phys. Lett.* **1995**, *247*, 210.

(23) An increase of the solvent polarity, e.g., from CBT to CBT/HFIP, enhances the thermodynamic driving force (Δ*G*) for an intramolecular electron transfer by lowering the energy of the respective charge-separated radical pair. Thus, upon addition of a protic cosolvent to CBT, a stronger luminescence quenching would have been expected also in the case of dyad **1**, reflecting the faster ET dynamics. The measured luminescence quantum yields in CBT/EtOH, CBT/TFE, and CBT/HFIP are, however, in sharp contrast to this trend, assuming no Marcus inverted behavior.

(1.76 eV)^{7a} or triplet state (1.5 eV)^{7a} to the ruthenium chromophore (1.98 eV)^{5e} can be neglected since the process would be endothermic.

Restoring the Donor–Acceptor Communication. After careful removal of HFIP from the 1:1 CBT/HFIP mixture by a nitrogen flow, the concentration of **1** was readjusted by adding CBT. The luminescence spectrum of **1**, now in 100% CBT, is superimposable on that previously recorded for the original CBT solution. This result suggests a refolding of the helical backbone as a consequence of the removal of the protic solvent component and a reactivation of the electron-transfer process. The HFIP addition–evaporation cycle was repeated 10 times, and the luminescence yield was checked after each step. A reproducible decrease of the luminescence yield (within 5%) was measured after each removal of HFIP. To further confirm the helical peptide triggering of the electron-transfer process, nanosecond photolysis was employed to monitor the presence of the ruthenium MLCT excited state in CBT/HFIP solution and the radical pair after removal of HFIP. Spectral features indicative of the ^{*}Ru²⁺-C₆₀ excited state and of the Ru³⁺-C₆₀^{•+} pair, respectively, were found that corroborate the luminescence data.

Conclusion

We have shown that solvent-dependent conformational changes of a peptide bridge, separating a ruthenium(II) trisbipyridine donor unit from a fulleropyrrolidine acceptor unit, dramatically influence the electron-transfer process that occurs in the [Ru(bpy)₃]²⁺/C₆₀ dyad **1** upon photoexcitation of the ruthenium chromophore. More specifically, addition of a strong protic solvent, such as HFIP, to a CBT solution of **1** disrupts the helical secondary structure of the peptide spacer that locates the Ru(II) and C₆₀ moieties to a distance which favors their mutual electronic interaction. We have also been able to demonstrate that this phenomenon is reversible.

The properties of HFIP as a solvent are well established.²⁴ In particular, its combination of high hydrogen-bonding donor strength and high polarity makes HFIP an ideal solvent to drastically increase the solubility of protected peptides in solution synthesis by disrupting self-associated β-sheet structures²⁵ and to spectroscopically study helical structure unfolding.^{3f,19,26} Mixtures of HFIP with chlorinated hydrocarbons are even more efficient than neat HFIP, as in this case the beneficial mechanism of heteroselective solvation (solvation in mixed solvents)^{25a} is operative. More specifically, one component of the solvent mixture (the chlorinated hydrocarbon) participates in van der Waals interactions with the peptide side chains, and the other component (HFIP) participates in hydrogen bonding to the peptide main chain.

Our results strongly support the view that, upon disruption of the 3₁₀-helical structure present in CBT by addition of HFIP, the separation between the two components, [Ru(bpy)₃]²⁺ and C₆₀, of the dyad **1**, located at the N- and C-termini of the peptide chain, tends to increase to a point that disfavors their mutual electronic interactions. This finding is not surprising in view of the characteristics of the 3₁₀-helix to be a relatively compressed ordered peptide secondary structure element, with the backbone φ and ψ torsion angles (−60°, −30°) much closer

to the cis than to the trans conformation.⁸ Therefore, it is reasonable to assume that an unfolding of this type of helix would result in a statistically unordered conformation characterized by larger absolute values of the average φ and ψ torsion angles and, consequently, by a greater average distance between the two termini. It is worth mentioning, however, that a variety of factors, other than through-space electronic interactions between the chromophores linked at the peptide N- and C-termini, could, in principle, affect the electron transfer. Disruption of the hydrogen bond network of the peptide backbone or preclusion of favorable conformational relationships that promote through-bond interactions by the protic solvent may contribute to deactivation of the electron transfer between the ruthenium and C₆₀ redox centers.

Experimental Section

General. Details regarding the instrumentation used in this work have been described elsewhere.^{7e,27}

Materials. C₆₀ was purchased from Bucky USA (99.5%). All other reagents were used as purchased from Fluka and Aldrich. (Boc-Ala)₂O²⁸ and *cis*-bis(2,2'-bipyridine-*N,N'*)dichlororuthenium(II) dihydrate²⁹ were prepared as described in the literature. All solvents were distilled prior to use. Dichloromethane, 1-chlorobutane, ethanol, 2,2,2-trifluoroethanol, 1,1,1,3,3,3-hexafluoro-2-propanol, 2-propanol, and acetone employed for UV–vis, steady-state luminescence, pico- and nanosecond flash photolysis, and pulse radiolysis measurements were commercial spectrophotometric grade solvents that were carefully deoxygenated prior to use.

Abbreviations. Symbols and abbreviations for amino acids and peptides are in accord with the recommendations of the IUPAC–IUB Commission on Nomenclature (*J. Biol. Chem.* **1972**, *247*, 977). The optically active α-amino acids are of L-chirality. Other abbreviations used are as follow: Z, benzyloxycarbonyl; Boc, *tert*-butyloxycarbonyl; OtBu, *tert*-butoxy; Aib, α-aminoisobutyric acid; NMM, *N*-methylmorpholine; HOAt, 7-aza-1-hydroxybenzotriazole; EDC·HCl, *N*-ethyl-*N'*-(3-dimethylaminopropyl)carbodiimide hydrochloride; Ac, acetyl; AcOEt, ethyl acetate; MeOH, methanol; AcOH, acetic acid; Ac₂O, acetic anhydride; TEA, triethylamine; DMSO, dimethyl sulfoxide; bpy, 2,2'-bipyridine; OTeg, triethyleneglycol monomethyl ether; TFA, trifluoroacetic acid; DCE, 1,2-dichloroethane; EtOH, ethanol; *n*-BuOH, *n*-butanol; CBT, 1-chlorobutane; HFIP, 1,1,1,3,3,3-hexafluoro-2-propanol; TFE, 2,2,2-trifluoroethanol; TEMPO, 2,2,6,6-tetramethylpiperidine-1-oxyl; R_f, TLC retention factor.

[Ru(bpy)₃]₂(L)](PF₆)₂ (1**).** A solution of bpy-Aib-Glu(OTeg)-Ala-Aib-Glu(OTeg)-Ala-3,4-fulleropyrrolidine (**L**) **2** (10 mg, 0.0056 mmol), Ru(bpy)₃Cl₂·2H₂O (3.5 mg, 0.0067 mmol), and NH₄PF₆ (89 mg, 0.055 mmol) in DCE (4 mL) was refluxed for 3 h under a nitrogen atmosphere. The solvent was removed in vacuo. The residue was loaded on top of a Sephadex LH-20 column and purified by gel filtration using CH₂Cl₂/MeOH 9:1 as eluant. The product was dissolved in the minimum amount of MeOH and precipitated by addition of toluene, affording 4.6 mg (33%) of **1**: IR (KBr) 3423, 1732, 1659, 1533, 1463, 845, 769, 576, 558, 528 cm⁻¹; ¹H NMR (CDCl₃) δ 8.64, 8.25, 8.04, 7.56 (4m, 27H), 5.60 (m, 4H), 5.20 (m, 1H), 4.08 (3m, 7H), 3.61 (m, 20H), 3.36 and 3.25 (2s, 6H), 2.46 (2m, 4H), 2.12 (m, 4H), 1.65–1.26 (m, 18H); UV–vis (CH₂Cl₂) λ (ε) 254 (45 200), 288 (47 300), 429 (5500), 486 (5900); MALDI-MS (MW = 2512) *m/z* = 2223 [M + H – 2PF₆]⁺. Amino acid analysis: Aib, 1.74; Glu, 2.26; Ala, 2.00.

Ligand (L) Bpy-Aib-Glu(OTeg)-Ala-Aib-Glu(OTeg)-Ala-fulleropyrrolidine (2**).** Bpy-Aib-Glu(OTeg)-Ala-Aib-Glu(OTeg)-OH **6** (see Supporting Information) (41 mg, 0.039 mmol) was dissolved in CH₂Cl₂ (5 mL) and cooled in an ice bath. HOAt (6.4 mg, 0.047 mmol),

(24) Ebersson, L.; Hartshorn, M. P.; Persson, O.; Radner, F. *J. Chem. Soc., Chem. Commun.* **1996**, 2105.

(25) (a) Narita, M.; Lee, J. S.; Hayashi, S.; Yamazaki, Y.; Sugiyama, T. *Bull. Chem. Soc. Jpn.* **1993**, *66*, 500. (b) Moretto, V.; Formaggio, F.; Crisma, M.; Toniolo, C.; Bodi, J.; Kimura, T.; Sakakibara, S. *Protein Pept. Lett.* **1995**, *2*, 275. (c) Nishino, N.; Xu, M.; Mihara, H.; Fujimoto, T. *Chem. Lett.* **1992**, 327.

(26) Parrish, J. R., Jr.; Blout, E. R. *Biopolymers* **1972**, *11*, 1001.

(27) (a) Bianco, A.; Bertolini, T.; Crisma, M.; Valle, G.; Toniolo, C.; Maggini, M.; Scorrano, G.; Prato, M. *J. Pept. Res.* **1997**, *50*, 159. (b) Bianco, A.; Maggini, M.; Scorrano, G.; Toniolo, C.; Marconi G.; Villani C.; Prato, M. *J. Am. Chem. Soc.* **1996**, *118*, 4072.

(28) Chen, F. M. F.; Kuroda, K.; Benoiton N. L. *Synthesis* **1978**, 928.

(29) Belsler, P.; Zelevsky, A. V. *Helv. Chim. Acta* **1980**, *63*, 1675.

EDC·HCl (11.2 mg, 0.058 mmol), and H-Ala-fulleropyrrolidine (29.6 mg, 0.032 mmol), the latter freshly prepared by a 4 N HCl treatment of Boc-Ala-fulleropyrrolidine **5** in dioxane followed by neutralization with NMM (5 μ L), were added, and the mixture was stirred at room temperature for 5 h. The solvent was removed in vacuo and the product purified by gel filtration on Sephadex LH-20 (eluant, CH₂Cl₂/MeOH 1:1). The product was dissolved in the minimum amount of CH₂Cl₂ and precipitated by addition of light petroleum, affording 43 mg (73%) of **2**: R_f (CHCl₃/EtOH 9:1) = 0.50; R_f (toluene/EtOH 7:1) = 0.10; IR (KBr) 3317, 1732, 1654, 1588, 1526, 574, 555, 526 cm⁻¹; ¹H NMR (CDCl₃) δ 9.20 (s broad, 1H), 8.72 (s broad, 1H), 8.56 (m, 4H), 8.35 (s broad, 1H), 8.04 (d, 1H), 7.98 (d, 1H), 7.88 (s broad, 1H), 7.36 (m, 3H), 5.50 (m, 4H), 5.14 (m, 1H), 4.60 (m, 1H), 4.22 and 3.95 (2m, 6H), 3.63 (m, 20H), 3.38 and 3.33 (2s, 6H), 2.68 (2m, 4H), 2.17 (m, 4H), 1.67–1.55 (m, 18H); ¹³C NMR (CD₂Cl₂/CS₂ 2:1) δ 175.45, 175.12, 175.00, 174.34, 173.16, 172.76, 171.62, 170.50, 166.52, 154.48, 154.11, 154.00, 153.62, 149.41, 148.60, 147.39, 146.34, 146.13, 145.72, 145.59, 145.35, 144.57, 143.09, 142.67, 142.32, 142.17, 141.96, 140.12, 137.17, 136.08, 128.81, 124.74, 121.74, 120.59, 72.00, 71.94, 70.66, 70.59, 70.50, 70.45, 69.18, 68.94, 64.35, 63.82, 63.68, 58.68, 58.62, 57.56, 57.16, 56.53, 30.97, 29.98, 27.21, 26.61, 24.89, 23.57, 23.52, 20.79, 17.44, 16.43; MALDI-MS (MW = 1808.9) m/z = 1832 [M + Na]⁺. Amino acid analysis: Aib, 1.78; Glu, 2.02; Ala, 2.20.

Ac-[Aib-Glu(OTeg)-Ala]₂-OrBu (3). Ac₂O (2 mL) was added to a solution of H-[Aib-Glu(OTeg)-Ala]₂-OrBu (0.16 g, 0.17 mmol), prepared by catalytic hydrogenation of Z-[Aib-Glu(OTeg)-Ala]₂-OrBu (see Supporting Information), in CH₂Cl₂ (2 mL), and the mixture was stirred at room temperature for 12 h. The solvent was evaporated under reduced pressure and the residue purified by flash chromatography (SiO₂; eluant, CHCl₃/MeOH 95:5), affording 0.11 g (65%) of **3** as an oil: R_f (CHCl₃/EtOH 9:1) = 0.40; R_f (*n*-BuOH/H₂O/AcOH 3:1:1) = 0.60; $[\alpha]_D^{20}$ = -16.1° (c 0.5, MeOH); IR (film) 3301, 1734, 1657, 1539 cm⁻¹; ¹H NMR (CD₂Cl₂) δ 8.17 (d, 1H), 7.89 (d, 1H), 7.30 (d, 1H), 7.15 (m, 2H), 6.46 (s, 1H), 4.34 and 4.17 (2m, 8H), 3.68 and 3.58 (2m, 20H), 3.38 (s, 6H), 2.56 and 2.45 (2m, 4H), 2.43 and 2.10 (2m, 7H), 1.56, 1.52, 1.48 and 1.46 (4s, 12H), 1.45 (s, 9H), 1.41 and 1.37 (m, 6H); MALDI-MS (MW = 979) m/z 1002 [M + Na]⁺. Amino acid analysis: Aib, 1.62; Glu, 2.06; Ala, 2.32.

[Ru(bpy)₂(L1)](PF₆)₂ (4). Bpy-[Aib-Glu(OTeg)-Ala]₂-OrBu (L1) (31.7 mg, 0.028 mmol) (see Supporting Information), Ru(bpy)₂Cl₂·2H₂O (17 mg, 0.033 mmol), and NH₄PF₆ (51 mg, 0.34 mmol) were dissolved in DCE (2 mL), and the mixture was refluxed for 3.5 h under nitrogen atmosphere. The solvent was removed in vacuo. The residue was purified by flash chromatography (SiO₂; eluant, CHCl₃/MeOH 8:2) and crystallized from CHCl₃/MeOH, affording 50 mg (96%) of **4**: R_f (CHCl₃/EtOH 9:1) = 0.05; IR (KBr) 3421, 3416, 1729, 1655, 1606, 1536, 1465 cm⁻¹; ¹H NMR (MeOD) δ 8.74, 8.62, 8.07, 7.80, 7.68, 7.46 and 7.26 (7m, 29H), 4.21 (m, 2H), 4.11 and 4.04 (2m, 6H), 3.59

and 3.47 (2m, 26H), 2.38 (m, 4H), 1.95 (m, 4H), 1.48–1.16 (m, 27H); MALDI-MS (MW = 1822) m/z 1533 [M + H - 2PF₆]⁺. Amino acid analysis: Aib, 2.15; Glu, 1.93; Ala, 1.92.

Boc-Ala-fulleropyrrolidine (5). A solution of C₆₀ (100 mg, 0.139 mmol), *para*-formaldehyde (15 mg, 0.5 mmol), and glycine (25 mg, 0.30 mmol) in toluene (30 mL) was refluxed for 2 h. The solution was loaded on the top of a SiO₂ column and purified by flash chromatography (eluant, toluene to remove unreacted C₆₀, then toluene/AcOEt 95:5). The solution containing the N-protected fulleropyrrolidine was concentrated to about 40 mL, cooled on an ice bath, and treated with (Boc-Ala)₂O (34 mg, 0.094 mmol), followed by addition of TEA (13 μ L, 0.094 mmol). The mixture was stirred at room temperature for 1 day, and then the solvent was removed in vacuo. The residue was purified by flash chromatography (SiO₂; eluant, toluene/AcOEt 95:5) and crystallized from toluene/CH₃CN, affording 13 mg (10%) of **5**: IR (KBr) 3422, 1705, 1662, 1447, 1247, 576, 526 cm⁻¹; ¹H NMR (CDCl₃) δ 5.50 (m, 5H), 5.02 (m, 1H), 1.66 (d, 3H), 1.49 (s, 9H); ¹³C NMR (CD₂Cl₂/CS₂ 1:1) δ 170.91, 154.72, 153.50, 153.03, 147.45, 146.44, 146.22, 145.73, 145.62, 145.56, 145.43, 144.58, 143.21, 142.79, 142.27, 142.20, 140.36, 135.98, 129.12, 128.36, 79.26, 71.00, 69.27, 66.00, 58.66, 57.34, 47.83, 47.74, 28.40, 19.58, 15.64; UV-vis (CH₂-Cl₂) λ (ϵ) 254 (125 000), 315 (39 900), 429 (4100); MALDI-MS (MW = 935) m/z = 958 [M + Na]⁺.

Acknowledgment. We thank Dr. R. Seraglia (CNR-Padova) for MALDI-MS data and Mr. V. Moretto for technical assistance. Part of this work was supported by CNR (*legge* 95/95) through the *Centro Meccanismi Reazioni Organiche* and by the Office of Basic Energy Sciences of the U.S. Department of Energy (Contribution No. 4087 from the Notre Dame Radiation Laboratory). M.M. and D.G. thank the NATO Collaborative Research Grants Program for a travel grant (Grant No. CRG960099).

Supporting Information Available: Synthetic details for the preparation of pentapeptides **6**, Z-[Aib-Glu(OTeg)-Ala]₂-OrBu, and bpy-[Aib-Glu(OTeg)-Ala]₂-OrBu (L1); 400-MHz ¹H NMR and FT-IR spectra of dyad **1**; FT-IR spectra of derivatives **2** and **3** (NH and CO stretching regions); ¹H NMR NH proton titrations of derivatives **2** and **3** using increasing amounts of DMSO-*d*₆; 400 MHz TOCSY, NOESY, and ROESY spectra of **2** and **3** in CDCl₃, DMSO-*d*₆, and CDCl₃/HFIP-*d*₂ 1:1 (PDF). This material is available free of charge via the Internet at <http://pubs.acs.org>.

JA983421D